

Distribution of salinity measurements and salinity variations on shelf- and in fjord waters, around Svalbard - throughout the last century



Jonas Darin

**Degree of Bachelor of Science
with a major in Earth Sciences
15 hec**

**Department of Earth Sciences
University of Gothenburg
2020 B-1092**

Faculty of Science



UNIVERSITY OF GOTHENBURG

Distribution of salinity measurements and salinity variations on shelf- and in fjord waters, around Svalbard - throughout the last century

Jonas Darin

ISSN 1400-3821

B1092
Bachelor of Science thesis
Göteborg 2020

Mailing address
Geovetarcentrum
S 405 30 Göteborg

Address
Geovetarcentrum
Guldhedsgatan 5A

Telephone
031-786 19 56

Geovetarcentrum
Göteborg University
S-405 30 Göteborg
SWEDEN

Abstract

Salinity data are an important component of the climate models that seek out to predict the climate variability. This data, of direct measurements, are scattered and needs to be assembled. This thesis set out to gather salinity data from the fjord and shelf area around Svalbard, to find out how the temporal and spatial distribution of data looked like. The waters around Svalbard are affected by both warm Atlantic water from the West Spitsbergen current, and colder Arctic water, flowing in a coastal current. Also, runoff from glaciers provides freshwater. Data were collected from the UNIS HD and EN4 database and were visualized. In addition, the gathered data were visually examined for anomalies and changes in the halocline depth over time. The resulting maps showed sparser amount of salinity data in the 1920's onwards with a major increase available data taking place in 1990's and from there on. The majority of the data are located on the west side of Svalbard. When investigating the change in Halocline over time, the visual method used, left room open for subjective interpretation. For this reason, this part was abandoned. Both low- and high salinity anomalies that stood out visually were selected. The high salinity anomalies are probably connected to the water intruding from the West Spitsbergen current, while one of the low salinity anomalies might be related to the melting of sea ice.

Table of Contents

1. Introduction	4
1.1 Water masses around Svalbard	6
1.2 Fjord hydrography.....	6
1.3 Intrusions of Atlantic Water upon the shelf	7
1.4 Aims and research questions	7
2. Methods	8
2.1 Data sources	8
2.2 Data management.....	8
2.3 Spatial distribution of data	8
2.3.1 Density Maps.....	8
2.3.2 Areas with CTD-profiles throughout the period of 1950-2019	8
2.4 Visualisation of Data.....	10
2.4.1 Halocline distribution	11
3. Results	11
3.1 Spatial and temporal distribution of CTD-profiles	11
3.2 Anomalies - When and where.....	13
3.3.1 High salinity events.....	15
3.3.2 Low Salinity events	18
4. Discussion	20
4.1 Spatial Distribution of CTD-profiles.....	20
4.2 Change in Halocline Depths	20
4.3 Salinity Anomalies	21
4.3.1 High Salinity events	21
4.3.2 Low Salinity Events	21
5. Conclusions.....	22
6. Acknowledgments.....	22
7. References	23
Appendix	26

1. Introduction

The Arctic sees a higher change in temperature compared to other northern latitude areas. This is the result of climate forcing and the effects are increased by positive feedback mechanisms. (Miller et al. 2010). The most important of these feedback mechanisms are the decrease in sea ice-, snow cover- and ice sheet extent. (Miller et al., 2010). Sea ice and fresh snow have a high albedo and thus, will reflect a large portion of the incoming solar radiation. When sea ice- and snow cover decreases, there is an increase in the amount of solar radiation absorbed, thus amplifying the warming even further. Furthermore, when sea ice is formed salt is rejected, which increases the salinity of the waters below; with this process being less frequent (Miller et al., 2010), it will add to the sea being less enriched with salt. The runoff of arctic glaciers and ice caps, especially the Greenland Ice sheet, has increased in recent years, providing more freshwater to the ocean (Dyurgerov et al., 2010; Hanna et al., 2005). In addition, anomalous years have caused extreme amounts of melting. (Tedesco et al., 2013). Where anomaly, in this respect, means something that stands out from the ordinary. Also, the river discharge into the Arctic Ocean has also been observed to increase (Peterson et al., 2002). To add to this, a freshening of the upper layer of the Arctic Ocean is predicted to continue in future years, creating a stronger stratification to the underlying halocline (Nummelin et al., 2016; Qi et al., 2017). These changes in salinity will likely have effects on water living organisms (Melnikov, 2005; Węśławski et al., 2010). Furthermore, if freshwater input into the Arctic Ocean and the north Atlantic increases, this might slow down the convection of the Meridional Overturning Circulation, possibly having global effects on the climate (Miller et al. 2010 and references therein). In addition, ocean salinity can be used to track changes in the water cycle, where evaporation and precipitation changes salinity of the water (Durack et al., 2012).

Salinity data can be used to evaluate the accuracy of climate models (Flato et al., 2013). However, long term salinity measurements in the Arctic Ocean is lacking. (Rhein et al., 2013 and reference therein). The available data of direct measurements need to be put together. Moreover, temporal and spatial gaps in this data need to be identified. Direct measurements are generally made with a Conductivity Temperature and Depth (CTD). A CTD is a device that can be sent down into water and measures the conductivity temperature and pressure throughout the water column, where the parameters for conductivity and pressure can be converted to salinity and depth.

The archipelago of Svalbard is located in the Arctic (Fig. 1), to the north of Norway and east of Greenland. The largest island in the archipelago is called Spitsbergen and its shelf and fjord areas are affected by a variety of water masses from different sources. The west coast of Spitsbergen is a place where exchange and mixing of waters originating from the Atlantic- and Arctic Ocean take place (Saloranta & Svendsen., 2001). In addition, the formation and melting of sea ice influence the water masses, along with runoff from glaciers and land. All these factors, mentioned above, will have an effect on the salinity of the waters on shelf and in fjord (Svendsen et al. 2002).

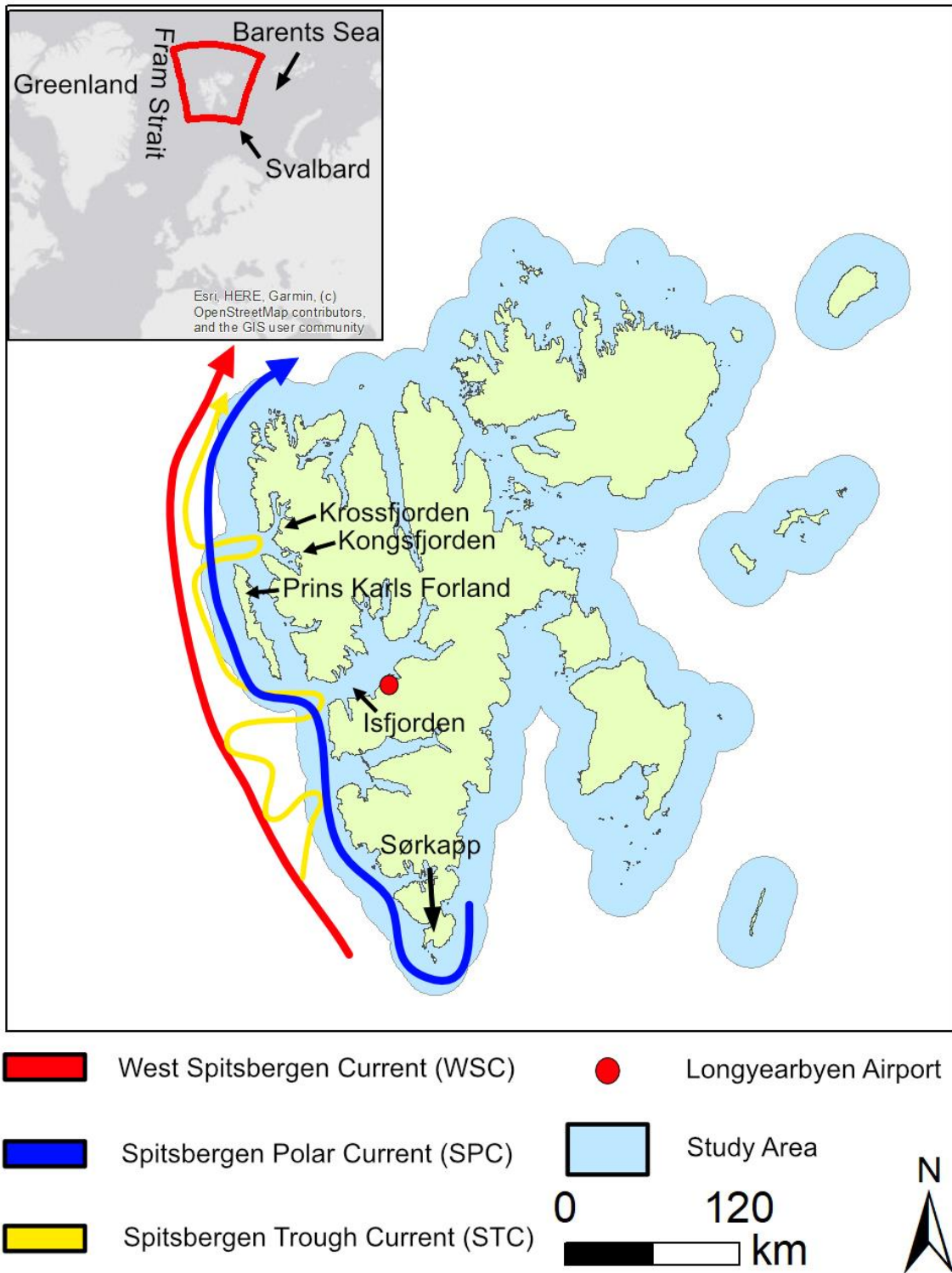


Fig. 1: Shows the Svalbard Branch of the West Spitsbergen Current, Spitsbergen Polar Current and Spitsbergen Trough Current. Also, the study area in blue and position of Longyearbyen Airport. Currents are modified from (Nilsen et al, 2016). (Sources: Svalbard map, ©Norwegian Polar Institute. Light Gray Map: Esri, DeLorme, HERE, MapmyIndia.)

1.1 Water masses around Svalbard

The Fram strait (Fig. 1), situated between Greenland and Svalbard is an important pathway for water-masses entering and exiting out of the Arctic Ocean. It contributes a great deal to the salt and heat exchange between the Atlantic- and Arctic Ocean (Gascard et al., 1995). In the eastern part of the strait, the West Spitsbergen Current (WSC) brings warm and salty Atlantic Water (AW) into the Arctic Ocean (Fig. 1). This current is a continuation of the Norwegian Atlantic current and follows the continental slope of Spitsbergen. When the current reaches the Yermak Plateau northwest of Spitsbergen it splits into two branches; where one of these, the Svalbard branch follows the upper continental slope, bypassing the plateau (Aagaard et al. 1987; Cokelet et al., 2008).

While the previously mentioned WSC runs along the slope of Spitsbergen, the Spitsbergen Polar Current flows upon the shelf (Fig. 1). This current transports Arctic Waters (ArW) from Storfjorden and the Barents Sea, to the west around the southern point of Spitsbergen and from there on north (Nilsen et al., 2016). On its way northwards, the ArW will be freshened by water exiting from the neighbouring fjords (Nilsen et al. 2008). The boundary between the warmer and more saline Atlantic water in the WSC on the continental slope and the colder and fresher ArW on the shelf mark out an oceanic front. This front is located in proximity to the shelf break where it occupies the near full depth of the water column, (Saloranta & Svendsen, 2001 and references therein) and is linked to the Polar Front that extends over the Barents Sea (Loeng, 1991).

The surface mixed layer is the uppermost layer of the ocean where various mixing processes make the temperature and salinity within the layer close to uniform. In the Arctic Ocean, the depth of the mixed layer is also influenced by the formation and melting of sea ice (Peralta-Ferriz & Woodgate, 2015). In the wintertime, as sea ice is formed, brine is rejected to the underlying water masses. This increases the density and leads to convection of these water masses, creating a deeper mixed layer. While in the summer, the melting of sea ice will create a thinner mixed layer. Although, during ice free conditions the winds can cause further mixing of this layer, deepening it (Peralta-Ferriz & Woodgate, 2015). However, strong stratification towards the underlying layer can inhibit this deepening from taking place (Peralta-Ferriz & Woodgate, 2015).

1.2 Fjord hydrography

The western part of Spitsbergen has an indented coastline, with a quite a few of these indentations being fjords. Three of these fjords are of interest in this study - Isfjorden, Kongsfjorden and Krossfjorden (Fig. 1), with the latter two sharing the same fjord entrance. These fjords have no shallow sills at the entrance and are connected to the shelf edge by troughs. All three fjords have glaciers that terminates into the sea and on land nearby. In Kongsfjorden the majority of the freshwater input comes from melting of snow and ice (Svendsen et al. 2002) and Nilsen et al. (2016) assume that most of the freshwater input into Isfjorden will be of glacial origin. This meltwater forms a low saline layer of Surface Water (SW), which often decreases in thickness in direction of the fjord mouth (Nilsen et al., 2008; Svendsen et al. 2002). This creates a stronger stratification during summer and autumn, than in spring and winter, when the stratification is often less defined. In Kongsfjorden, as meltwater is added into the fjord it will create a flow of surface water out of the fjord, which in turn, leads to water of Atlantic Water (AW) or Intermediate Water (IW) masses entering the fjord at a greater depth. (Sundfjord et al., 2017). Intermediate Waters often form through mixing of SW with the underlying water and thus often occupies the space between the SW and more dense water masses. (Svendsen et al., 2002)

Cooling of the SW results in Local Water (LW) being produced (Nilsen et al., 2008). As LW freezes and sea ice is formed, brine is rejected to the underlying waters and dense Winter Cooled Water (WCW) is created. This will lead to convection of the dense water and further mixing of the water column. For this process the fjord polynyas (open waters surrounded by sea ice) are important, as they function as ice factories (Nilsen et al., 2008).

1.3 Intrusions of Atlantic Water upon the shelf

Winds from the south will cause an Ekman transport to east and lead to water piling up against the west Spitsbergen coastline, raising the sea surface elevation. As a result, it will cause the barotropic driven WSC to speed up and shift eastwards (Nilsen et al., 2016). When this happens AW from the WSC will be topographically guided upon the west Spitsbergen shelf in system of troughs, Spitsbergen Trough current, that eventually ends up in the Arctic Ocean (Nilsen et al., 2016). If the shift is small AW will run in and out of the Isfjorden trough; when the shift is greater AW will also flow through Kongsfjorden trough, and the entire west Spitsbergen shelf can be affected by the warm water (Nilsen et al., 2016). However, the flow of the SPC is strengthened during these circumstances and will act as barrier from AW entering Isfjorden, and occasionally Kongsfjorden (Nilsen et al., 2016; Sundfjord et al., 2017). When the wind dies or changes direction to northerly, the surface water that have been piled up at the coast from the southerly winds will move west. This will lead to a compensation current and upwelling from deeper waters with AW (Cottier et al., 2007; Nilsen et al., 2016). Under these conditions with northerly winds it will be possible for AW to enter Isfjorden (Fraser et al. 2018). When AW enters shelf and fjord environment it will mix with ArW, creating Transformed Atlantic Water. This is slightly colder than the original water and has a lower salinity due to mixing (Nilsen et al 2008; Svendsen et al. 2002).

Nilsen et al. (2016) relates the intrusion of AW upon the shelf to cyclones passing by in the Fram Strait, these giving rise to the southerly winds. These intrusions will influence the coverage of sea ice in shelf and fjord areas (Cottier et al., 2007; Nilsen et al., 2016). Also, Luckman et al. (2015) found sea water temperature at depth to be the most important factor for frontal ablation of, studied Svalbard glaciers that terminates in the sea.

1.4 Aims and research questions

The aim of this thesis is to evaluate the distribution of historical salinity recordings in coastal waters around Svalbard. I have gathered data from available databases and used relevant literature to detect potential variations in the salinity. This material has been used to answer the following research questions:

- How has the halocline distribution within fjord and shelf area shifted in the last century?
- Where can we find spatial or temporal gaps in the recordings?
- Can any specific salinity anomalies be identified during this period, if so, what can they be related to?

2. Methods

2.1 Data sources

Data for CTD-measurements, with salinity readings, were acquired from two different sources. The majority gathered from the UNIS Hydrographic Database (UNIS HD), (Skogseth et al., 2019) and a minor part collected from the EN4 Database (Good et al., 2013). The UNIS HD is collaboration between several different contributors. These include Norwegian Universities and authorities, among others. This dataset covers measurements from all around Svalbard between 0-34°E and 75-83°N. The EN4 Database is constructed by the Met Hadley Centre of Observations, mainly with data from World Ocean Database. Data used from this database are made up of measurements in the area around Isfjorden (Fig. 1). Meteorological data from Longyearbyen Airport was collected from the Norwegian Meteorological Institute (Norwegian Meteorological Institute, 2020). A map of Svalbard (©Norwegian Polar Institute) was downloaded from the Norwegian Polar Institute (Norwegian Polar Institute, 2020).

2.2 Data management

The data from UNIS HD were in NetCDF format, where each file corresponds to a CTD profile at a certain time, latitude, and longitude. Accompanying these values are multiple recordings of salinity, temperature, and pressure. There was a considerable amount of data to go through, and doing it manually was not an option. For this reason, several scripts were created, using MATLAB R2019B, to help with – data import, sorting, and visualisation. For greater detail, the four scripts mainly used can be found in the appendix of this report, with comments.

2.3 Spatial distribution of data

The study area was decided to extend 22 km from land, being the same as the Territorial sea. This area was marked as a surface and CTD-profiles outside of this area were removed.

2.3.1 Density Maps

To look at differences in the spatial distribution of CTD-measurements through the last century, point density maps were created in ArcGIS 10.7.1. The tools used in the process of making these maps are described below. To start with, data were imported from both data sets. The data from the UNIS HD came in the format per CTD-profile. While the data from the EN4 database were provided as a continuous list of depth and salinity values, and there was no easy way to distinguish between the CTD-profiles. Instead, every 10 m value was extracted to represent a CTD-profile, because this seemed to be a common depth present in the profiles. The data were divided into three time periods, this was done on the basis that the periods shared some spatial characteristics. The data were converted to a projected coordinate system and the points that extended more than 22 km from land were removed. Afterwards, kernel density tool was used, and search radius was set to 8 km. This amount of generalization seemed like a reasonable choice for getting a good overview. However, some amount of detail will be lost. Finally, area extended outside the study area was removed.

2.3.2 Areas with CTD-profiles throughout the period of 1950-2019

To help find the places where CTD-profiles were available from year 1950-2019 - ArcGIS 10.7.1 was used. This was a rather computer-heavy task, and for this reason year 1920-1949 were excluded from the analysis, as previous visual examination had shown the amount of CTD-profiles sparse from this

period. Instead, year 1950-2019 was divided in to 10-year periods and the output of the analysis, were the areas, where at least one CTD-profile from each ten-year period had been taken. To deal with problem of CTD profiles not being taken exactly in the same location, a circle with a certain radius is drawn, forming a surface. This was done prior to running the analysis. The workflow of all these steps can be seen in Fig. 2.

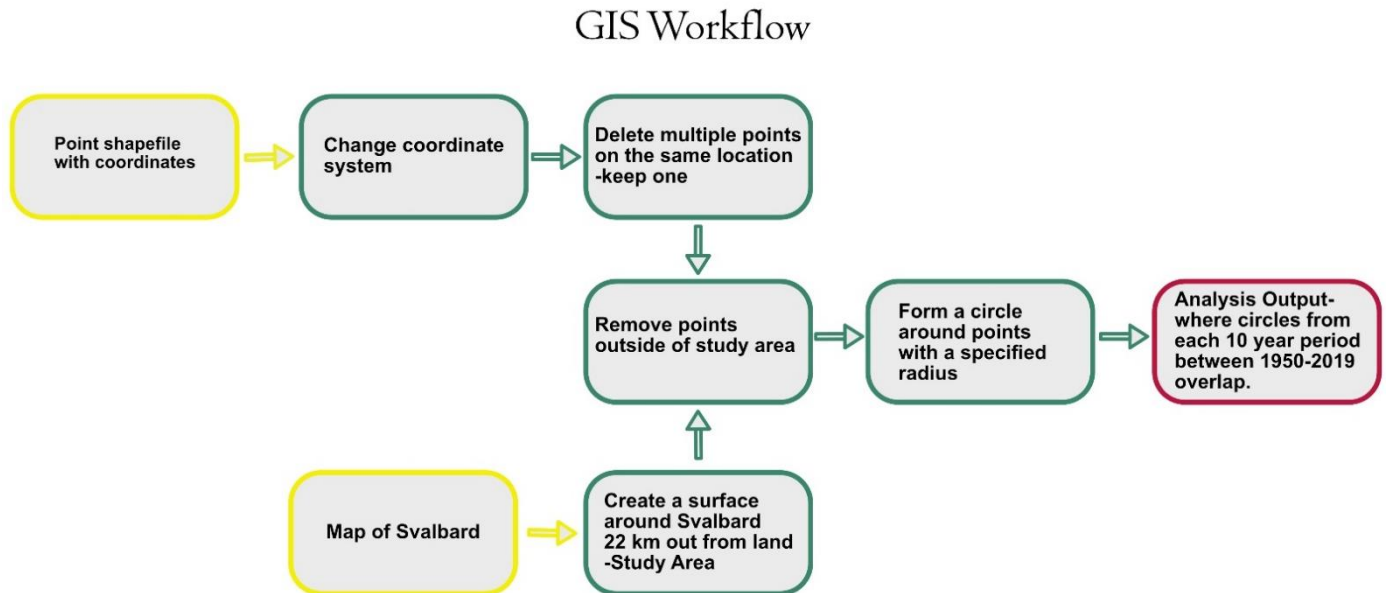
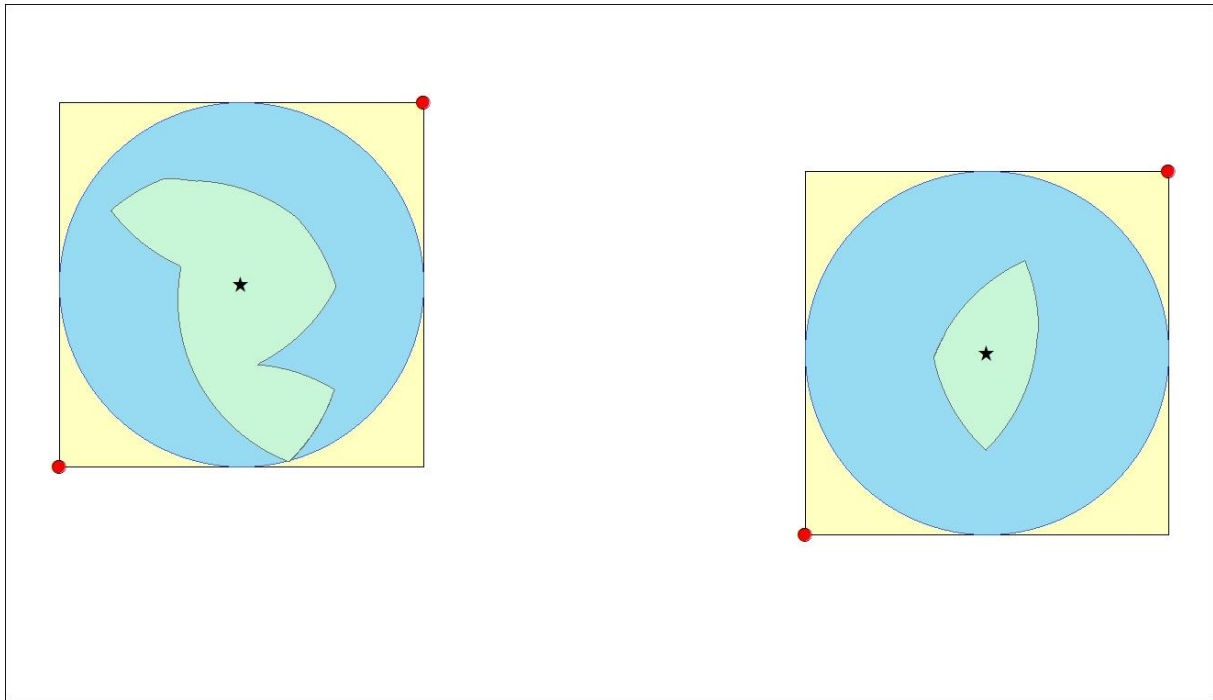


Fig. 2: Workflow used in GIS.

The next step was to create a Latitude and Longitude interval from the analysis output, the overlapping areas for the 10-year periods between 1950-2019. An explanatory picture of this workflow can be seen in Fig. 3. To begin with, a point was placed on each of the output surfaces. If the chosen radius (previously mentioned above) had been 2 km, a circle with a radius of 2 km is created around the points. These circles contained all of the CTD-profiles from the analysis output. After this, a square was fitted to the edges of the circle. From now on, these areas will be referred to as Intersect areas. Finally, points were placed in the southwest and northeast corner. This gave a latitude and longitude interval of the area in the square and was exported as a table with coordinates.



- | | |
|---|---|
| 1. Analysis Output | 4. Intersect Area |
| 2. Manually inserted point | 5. Points to get Lat and long interval of Intersect Area |
| 3. Buffer | |

Fig. 3: Shows the steps to create the latitude and longitude intervals. This was done by creating a buffer that includes CTD-profiles from the Analysis output. To be able to export these as coordinates a square was fitted around the circle and marked with points at the ends. (Sources: Created using ArcMap 10.7.1)

2.4 Visualisation of Data

The coordinates with the latitude and longitude intervals were used with the scripts to extract the corresponding CTD-data within this interval (MATLAB R2019B). There were 11 different areas, defined by the intervals from the previous analysis and the scripts were run on each of these successively. When converting decibars into depth in meters, using equations from Fofonoff & Millard (1983) the difference from converting decibars straight into meters, were relatively small at shallower depth, around 1 m difference at 100 m depth. For this reason, a conversion between decibar and depth [m] was done at a 1:1 ratio.

Script #2 generated 2D-graphs of salinity (or temperature) against depth for every CTD-profile inside the interval and saved each of these as an image with latitude, longitude, and date as a title.

Script #3 selected data inside the latitude and longitude interval and plotted it as surface plot of time, depth, and salinity (or temperature). To be able to handle the issue with time and depth variables for the CTD-profiles not being evenly spaced, meshgrid and griddata functions were used before plotting it as a surface. Meshgrid creates a grid for a specified interval of chosen time and depth. Griddata will create an interpolated surface using the meshgrid-output and time, depth and salinity variables. On the interpolated surface every time- and depth value from the meshgrid will

correspond to an interpolated salinity value. The interpolated surface will always run through the actual values. (Mathworks, 2020) To show where these actual values are located a 3D scatter plot was placed upon the surface plot. This helps to interpret the areas where the interpolation is likely to be more correct and where it is probably wrong, with longer distance from an actual value.

Both surface plots and 2D plots (MATLAB R2019B) were created and used to identify anomalies, within the 11 different areas. These were selected from the values that stood out the most visually, from the surface waters. When an anomaly was identified, the date of it happening was inserted into Script #4. This script collects all the profiles from a date within a chosen latitude and longitude interval. Afterwards, the acquired CTD-profiles were plotted as transects in Ocean Data Viewer 5.2.0. with maps created in ArcGis 10.7.1 using the Svalbard map (©Norwegian Polar Institute). This was done to be able to see if the anomalies were of local or larger scale. To classify the water masses shown in the transects the classification from Nilsen et. (2008) and Svendsen et al. (2002) was used.

Table 1: Classification of water masses according to (Nilsen et al., 2008; Svendsen et al. 2002).

Water mass	Salinity [psu]	Temperature [°C]
Atlantic Water (AW)	>34.9	>3
Intermediate Water (IW)	34-34.7	>1
Local Water (LW)	~34	<1
Surface Water (SW)	28-34	>1
Transformed Atlantic Water (TAW)	>34.7	>1
Winter Cooled Water (WCW)	>34.4	<-0.5

2.4.1 Halocline distribution

To evaluate the change of the halocline distribution over time a slightly smaller area was used, compared to when looking for anomalies. This area was a square with an area of around 10km². The reason for this was to keep variations due to location relatively small, but still have enough CTD-profiles to look at. This yielded six intersected areas and script #2 was run at all of these to generate 2D plots of salinity and depth. To avoid mixing in the seasonal halocline changes into the calculations, profiles taken during September-October were chosen. Also, profiles with a resolution greater than 5 m was discarded. Since the halocline often extended for many meters vertically, the top of the halocline for each plot was recorded. Due to sparse coverage of CTD-profiles and low vertical resolution from the earlier years of the studied period, this analysis was abandoned.

3. Results

3.1 Spatial and temporal distribution of CTD-profiles

As can be seen in Fig. 4 there is noticeable difference in the amount of CTD-profiles taken between year 1920-1959 and 1960-1989. While the difference of these two periods compared to 1990-2019 is even more pronounced with a major increase in CTD-profiles in the latter one. In the two earlier time periods the location with most frequent measurements is the area around Isfjorden and Sørkapp. In the 90's there is a shift towards more CTD-profiles in Isfjorden-, Kongsfjorden area. A major difference in the amount of profiles taken can also be seen between the east and west side, throughout all time periods. In fig. 5 this also noticeable for the areas with CTD-profiles from year 1950-2019, as all these locations are on the west coast of Spitsbergen. The figure shows the results with the 2 km radius, as was described in methods.

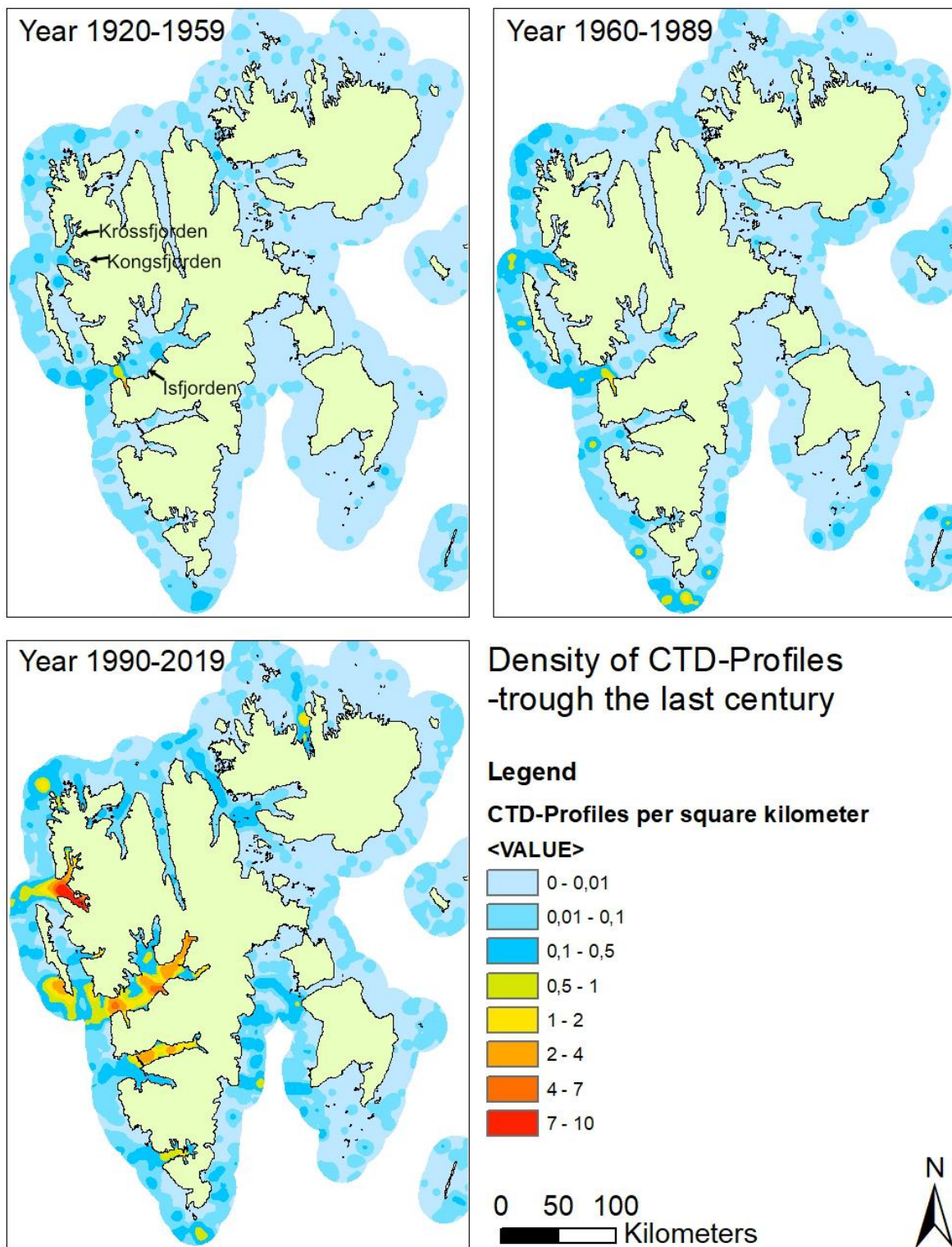


Fig. 4: Shows sample density in CTD-profiles per square kilometre during three different time periods – 1920-1959, 1960-1989, and 1990-2019. (Sources: Svalbard Map, ©Norwegian Polar Institute.)

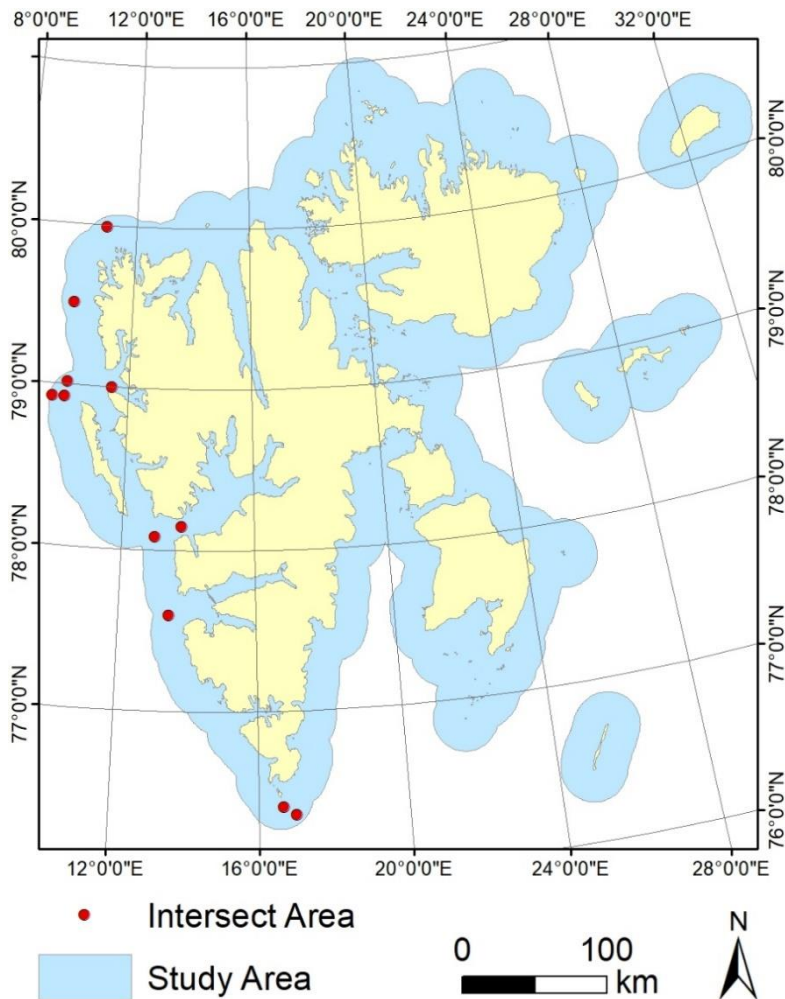


Fig. 5: Shows the Intersect Areas, which are the locations where CTD-profiles from 10-year periods between 1950-2019 overlap . (Sources: Svalbard Map, ©Norwegian Polar Institute.)

Salinity anomalies

3.2 Anomalies - When and where

Surfaceplots with identified salinity anomalies can be seen below. To be able to see anomalies more clearly, the view is zoomed in, which results in some profiles disappearing out of view. Also, note that the scale of the colorbar for salinity will change between the figures. Only the anomalies that stood out the most visually were selected.

Low salinity anomalies can be seen in August 1993 and 2004. The 1993 anomalies is visible in Isfjorden(Fig. 6c) but also to the north (Fig. 5, two northern most points) In 2004 anomalies can be seen in Isfjorden (Fig. 6c) and Kongsfjorden (Fig. 6a) at the same time (It is not the anomaly extending all the way down in Fig. 6a, this anomaly was only found in one CTD-profile and therefore was not included in the report.)

High salinity anomalies were found in September 1973, may 2007 and 2014. The 1973 anomaly is visible NW of Prins Karls Forland (Fig. 6b). The 2007 anomaly is visible in Kongsfjorden(Fig. 6a) and

NW of Prins Karls forland (Fig. 6b) at the same time. The 2014 anomaly can be seen at Sørkapp (Fig. 1) and in Kongsfjorden about the same time.

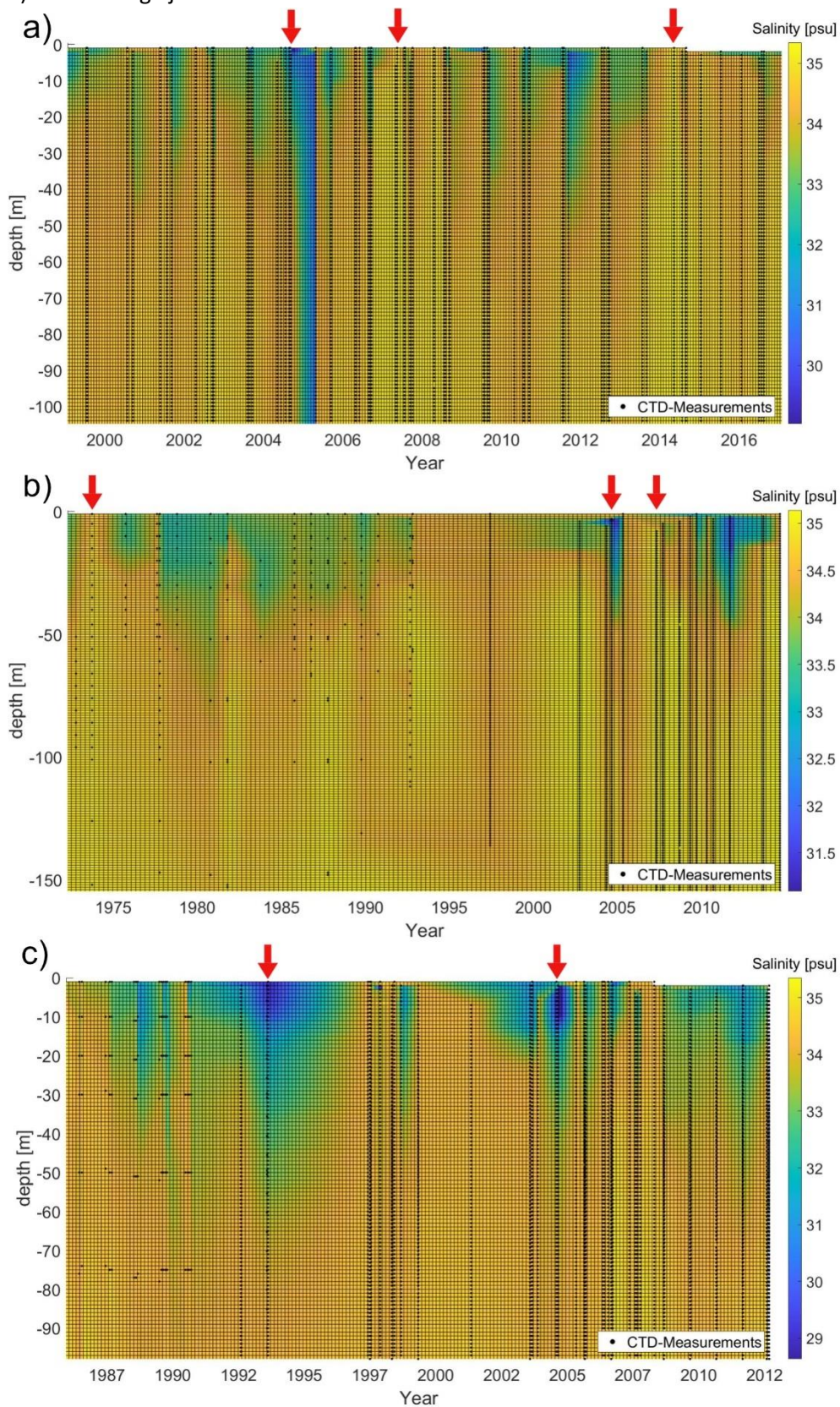


Fig. 6: Change in salinity with depth and over time, with salinity as a coloured surface, time at x-axis, and depth at y-axis. Black dots show positions of actual CTD-measurements and red arrows points toward identified anomalies. Anomalies shown for a) Kongsfjorden (from August 2004, May 2007 and

June 2014. b) NW of Prins Karls Forland from September 1973, august 2004 and may 2007 c) Isfjorden from August 1993 and August 2004

3.3 Transects

The following transects are linked to the anomalies shown above, from CTD-profiles in the same areas and dates when the anomalies were found. These were made to visualize the extent of the anomalies and see if they were of larger or smaller scale, when seen in the context of other CTD-profiles nearby. Anomalies that only were found in a single CTD-profile are were discarded and are not shown below.

3.3.1 High salinity events

Atlantic Water occupies near the full depth of the water column to west in Fig. 7, freshening towards the coast is observed. Additionally, in the eastern part of the profile a shift towards TAW and followed by IW can be seen.

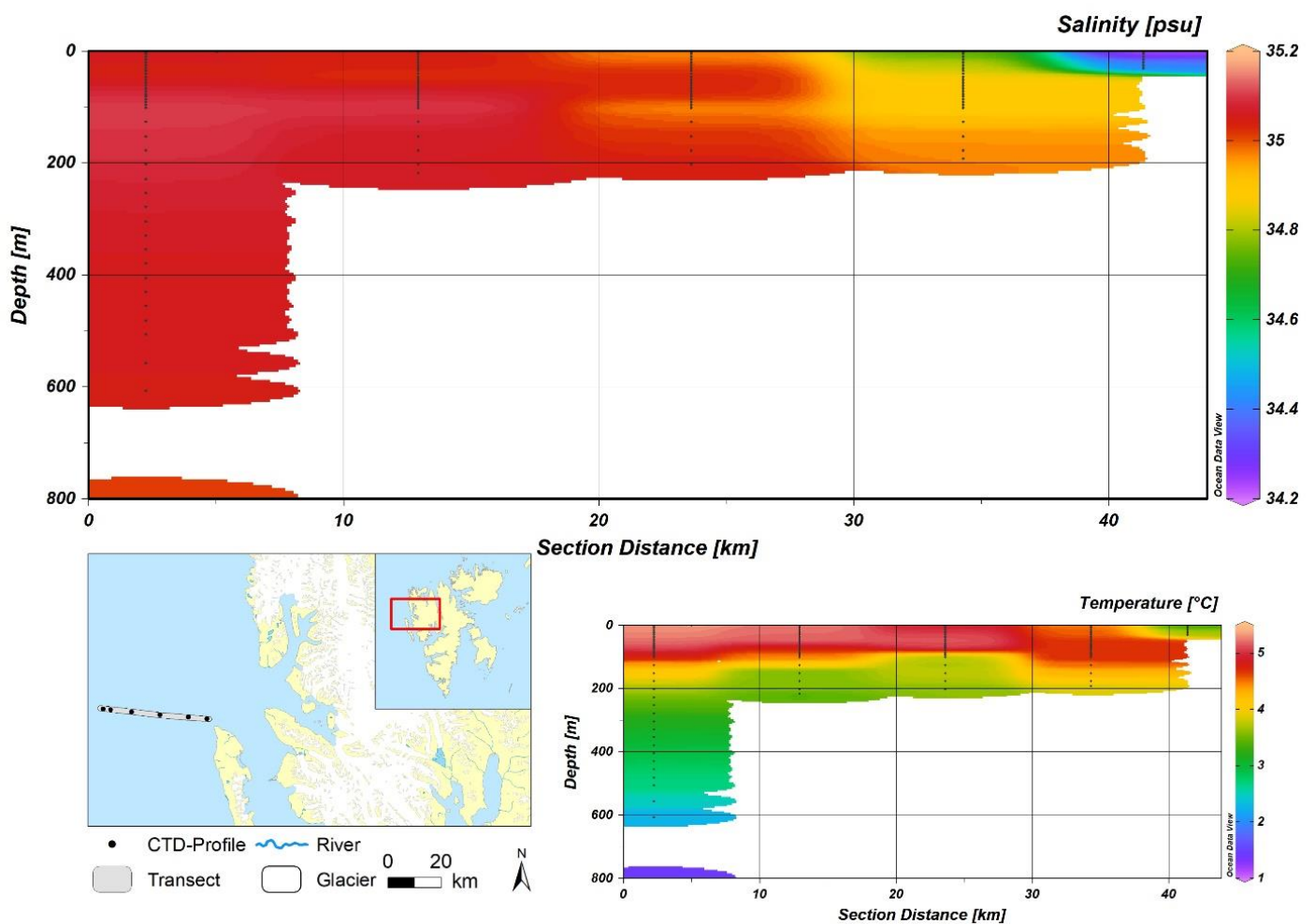


Fig. 7: Transect of CTD-profiles taken north west of Prins Karls Forland 1973-09-22 showing Salinity [psu] in the upper chart and Temperature [°C] in the lower chart. In the lower left corner is map showing the transect and the CTD-profiles as points.

Atlantic Water and Transformed Atlantic water can be seen occupying the majority of the water column (Fig. 8), generally AW is found closer to the surface with TAW beneath. A fresher spot that also stands out temperature-wise can be seen at close to the entrance of Kongsfjorden, this water still qualifies as TAW though, because of relatively high temperature and salinity.

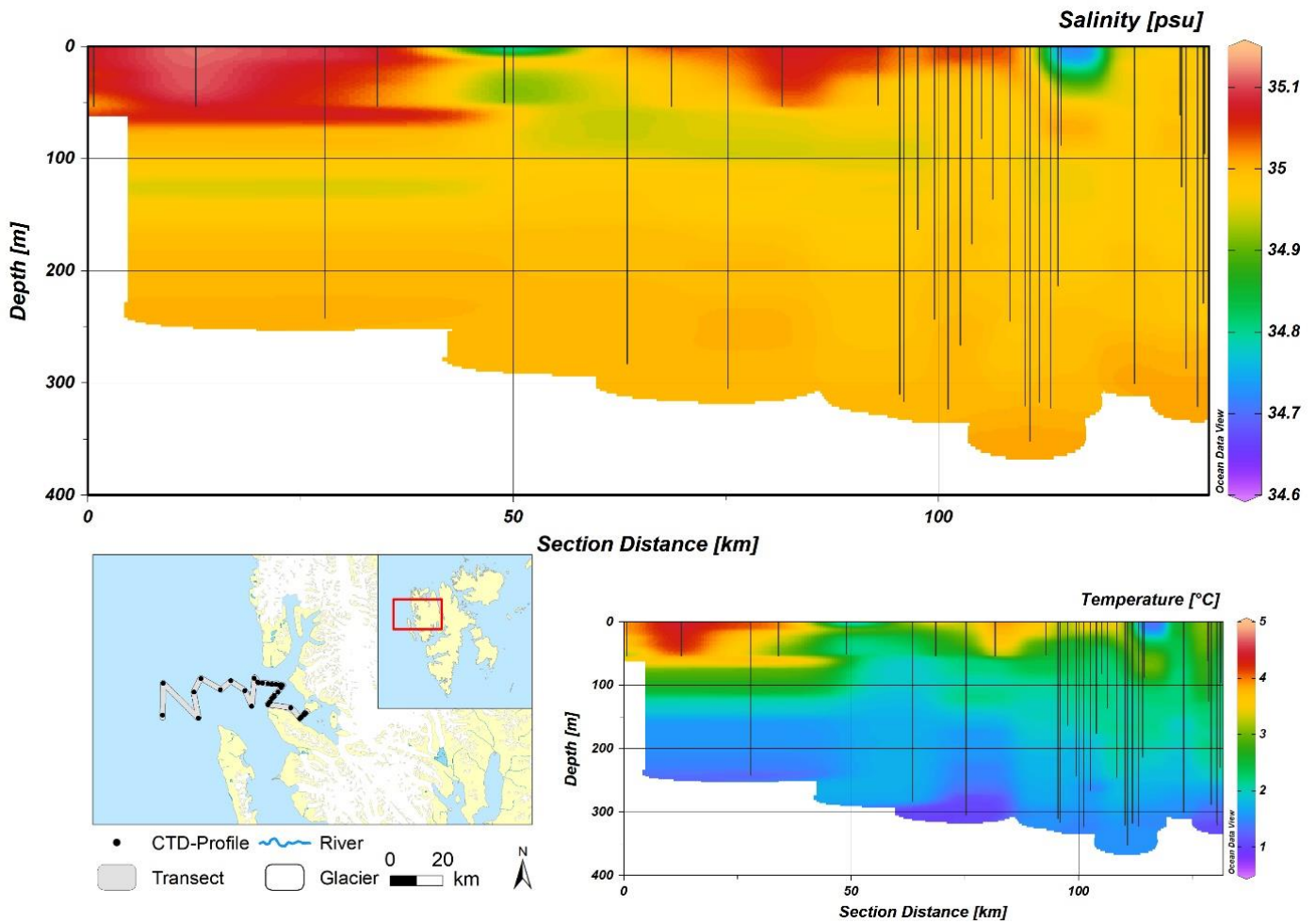


Fig. 8: Transect of CTD-profiles taken in west of and in Kongsfjorden 2007-05-13 – 05-16, showing Salinity [psu] in the upper chart and Temperature [°C] in the lower chart. In the lower left corner is map showing the transect and the CTD-profiles as points.

The SW reaches down to about 20 m below the surface and the upper layer becomes fresher into the fjord (Fig. 9). Below is gradual transition from IW, to TAW into AW. Beneath the AW in the western part of the transect, close to the bottom, the water defines as TAW again, this is due to lowering in temperature. The water still retains a salinity over 35.

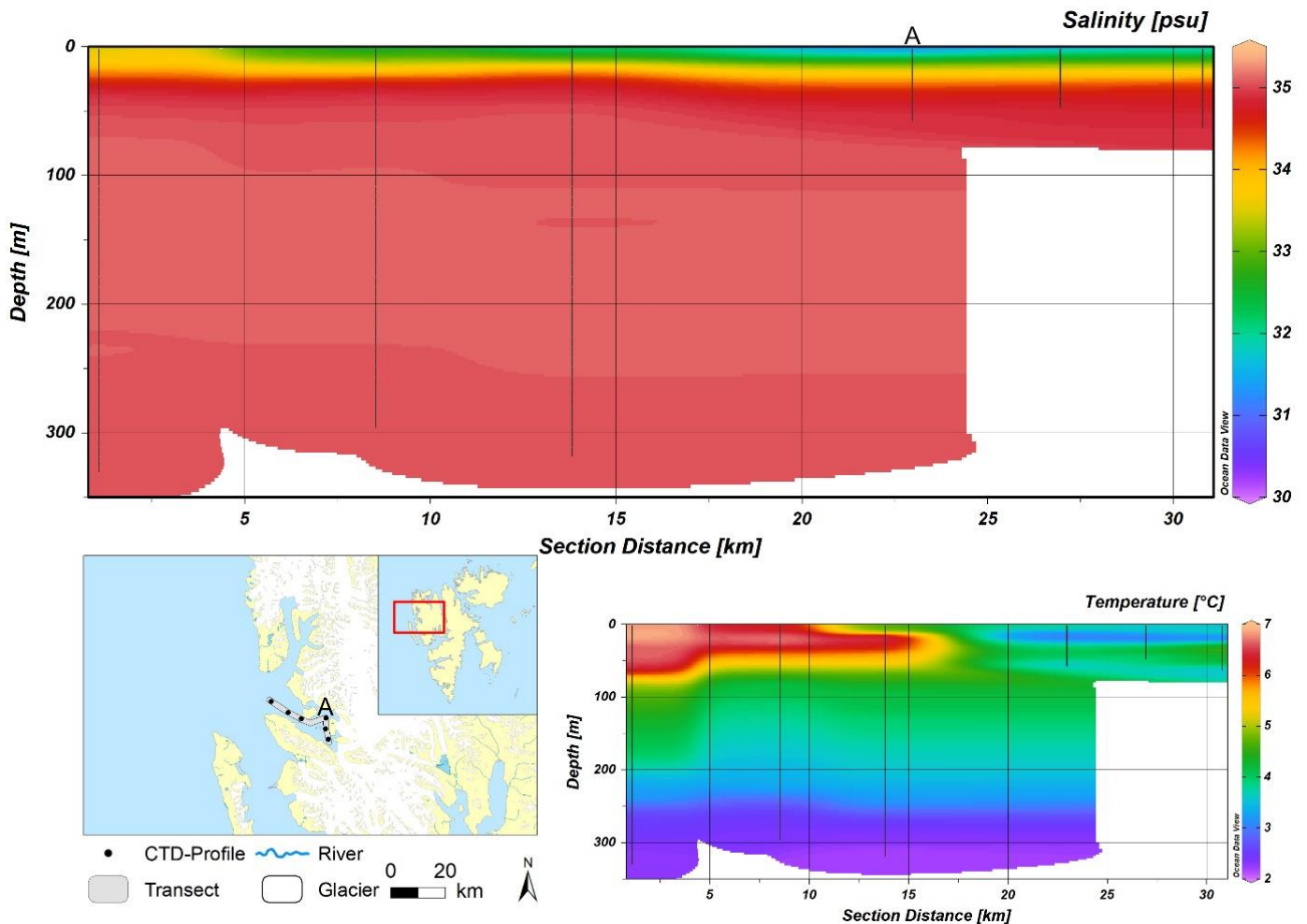


Fig. 9: Transect of CTD-profiles taken in Kongsfjorden 2014-07-23, showing Salinity [psu] in the upper chart and Temperature [°C] in the lower chart. In the lower left corner is map showing the transect and the CTD-profiles as points.

3.3.2 Low Salinity events

The Surface waters roughly occupies the upper 60 m of the water column (Fig. 10) and a gradual decrease in salinity can be seen. It can also be noted that the water is fresher in the middle of transect and furthestmost to east. Below this at the eastern side, are masses of LW and WCW at the temperature minimum. On the western below the SW, masses of IW and TAW are observed with the higher temperature compared to LW and WCW. TAW can also be seen the deepest part of the transect.

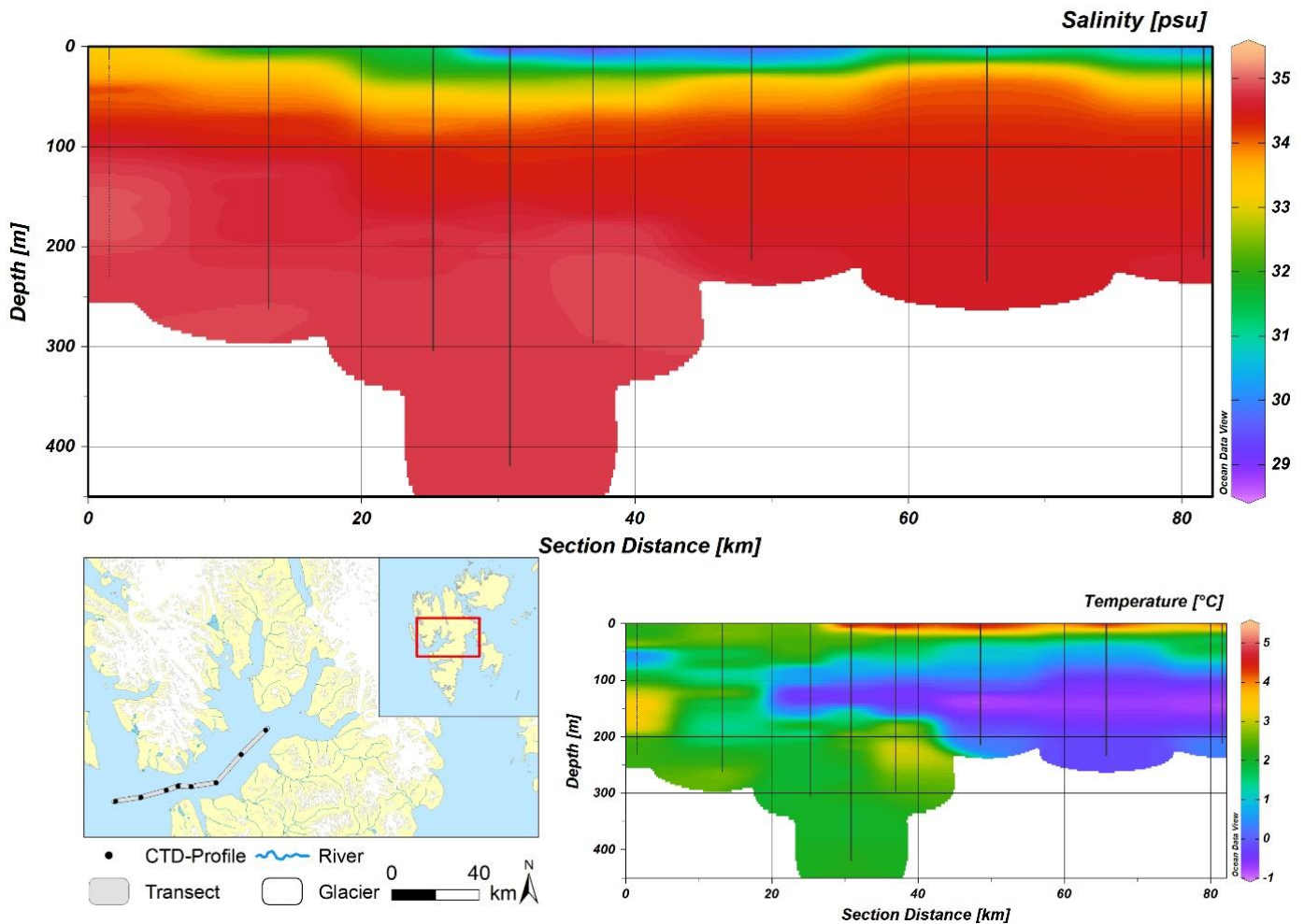


Fig. 10: Transect of CTD-profiles taken in Isfjorden in 1993-08-15, showing Salinity [psu] in the upper chart and Temperature [°C] in the lower chart. In the lower left corner is map showing the transect and the CTD-profiles as points.

Surface Waters occupies the water column down to roughly 30-50 m depth (Fig. 11) and a gradual decrease in salinity is observed vertically. Also, freshening towards the north shore can be seen. Below the SW a layer of LW can be seen throughout the entire transect. Beneath this along the southern shore are layer of IW. In contrast to this, there is a layer of WCW in the northern part. The bottom waters hold IW, more saline than the waters above.

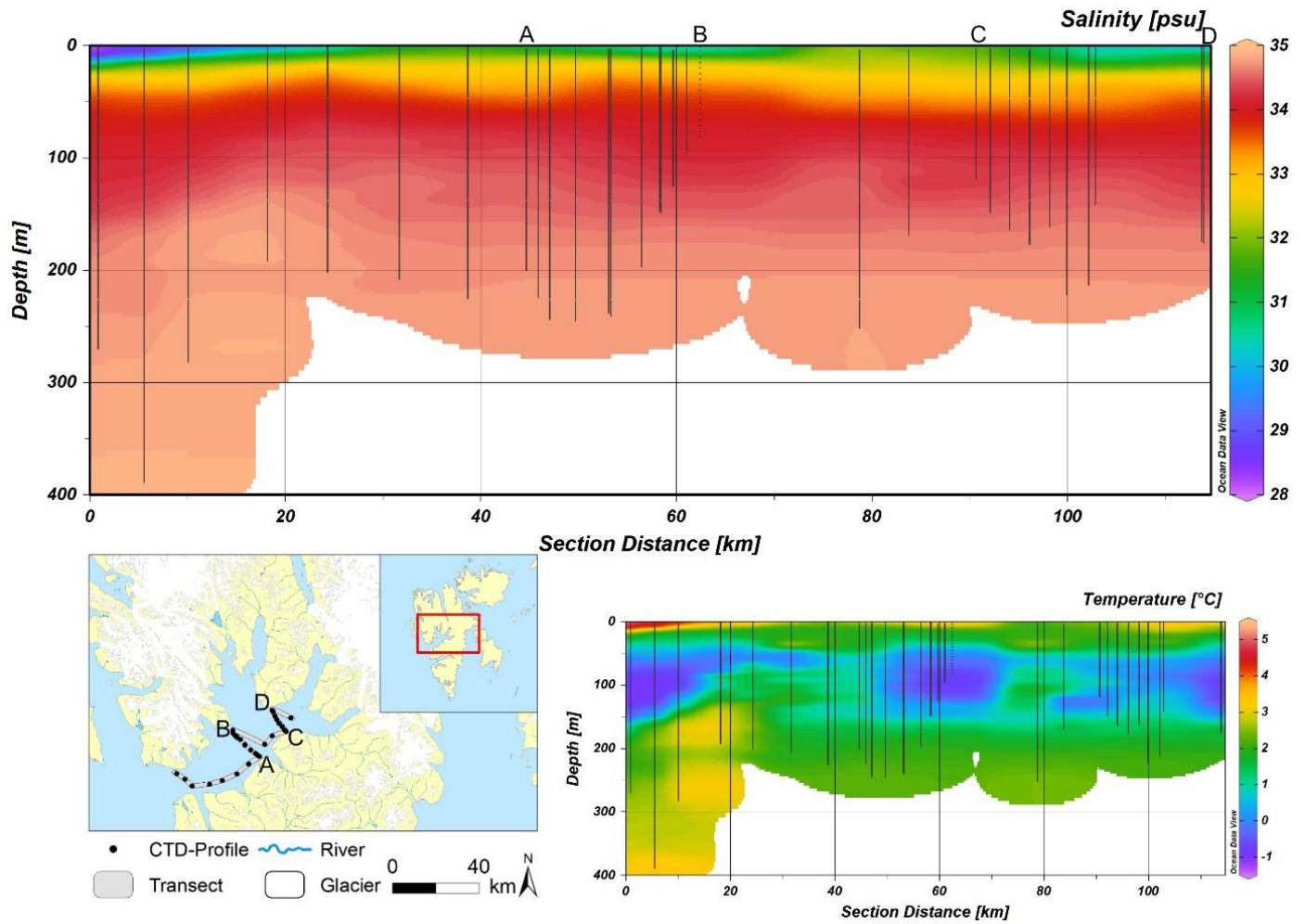


Fig. 11: Transect of CTD-profiles taken south of Isfjorden 2004-08-29 , showing Salinity [psu] in the upper chart and Temperature [°C] in the lower chart. In the lower left corner is map showing the transect and the CTD-profiles as points.

4. Discussion

4.1 Spatial Distribution of CTD-profiles

From what can be seen in Fig. 4, it is noticeable that data are scarce before year 1950, afterwards the number of CTD-profiles increases slightly, but it is not until the early 90's when major increase in CTD-profiles taken can be seen. The studies that spans over longer time periods seems to be few in numbers and in one of them that do, (Pavlov et al. 2013), data is observed to be sparse before the mid 80's. While many of the studies, using salinity data, have a study period that last for a couple of years, e.g. (Cottier et al., 2007; Nilsen et al., 2008; Svendsen et al., 2002). Generally, it seems to be difficult to find locations with many available CTD-profiles, through a longer time period, before year 1990. This might cause difficulties since salinity measurements are of importance for climate modelling (Delcroix et al., 2011 and reference therein; Durack et al., 2012). Also, in Fig. 5 it is visible that all the areas where CTD-profiles have been taken throughout year 1950-2019, are all on the west side. This might be because of the major settlements on Svalbard all being located on the west side, along with sea ice often being present on the eastern side. Where the western coast is often free of ice due to the WSC (Svendsen et al., 2002) so it is likely more accessible. Data is also more concentrated off the coast with relatively few points within a Nautical mile from the shore. Possibly, because it is difficult for the ships, that do these measurements, to navigate closer to the shore. Also, it is important to mention that only data from two databases, UNIS HD and EN4 databases, have been examined closer. The search for data was stopped there due to the large amount of data found within these databases.

What was seen when looking at the CTD-profiles from these places, of CTD-profiles throughout year 1950-2019; was that there in many cases only was one or two measurement for a certain 10-year period, which was often the case in earlier years. This was a problem with the method used, because there only needed to be one CTD-profile, within each 10-year interval between year 1950-2019, for it to pass as an intersect area. However, this might also mean that areas that have CTD-profiles in 6 out of 7 time periods were disregarded, which possibly could have made good areas for study. Aside from the problem with the earlier CTD-profiles being less in number, these also have lower vertical resolution between the measurements. Many of the earlier CTD-profiles have 10 m or more between the measurements, and this continues into the 80's on some profiles.

4.2 Change in Halocline Depths

Due to the difficulties when trying to assess the change in halocline depth, throughout the last century, I decided not to go through with analysis. Many of the earlier CTD-profiles was discarded because of the low vertical resolution (>5m) between measurements, this made the difference even more pronounced between earlier- and late CTD-profiles. Deciding where the halocline starts was also more difficult with 5 m vertical resolution compared to 1 m, and left a lot of room for subjective interpretation, possibly making the error even greater. To be able to remove this subjective judgement, with a choice of a different method would have been beneficial. When assessing the depth of the mixed layer throughout the arctic ocean, Peralta-Ferriz & Woodgate (2015) used an increase-in-density criterion for defining the mixed layer depth. Generally, for the arctic ocean the mixed layer is overlying a cold halocline (Rudels et al., 1996). While for the shelf area Saloranta & Svendsen (2001) describes the uppermost layer of the water column as fresher layer that thickens towards the shore, overlying a halocline. For these reasons, it seems likely that the mixed layer depth will coincide with the halocline and that Peralta-Ferriz & Woodgates (2015) method also can be used

for halocline depth. If that is not the case, maybe a certain amount of increase in salinity could be used to define the halocline instead.

4.3 Salinity Anomalies

4.3.1 High Salinity events

From what can be seen in Fig. 7, almost the entire water column is filled with Atlantic Water (AW), salinity over 34.9 and temperature above 3°C. This water is very likely to origin from the WSC judging by its high salinity and temperature, as defined in (Svendsen et al. 2002) and has probably been transported upon the shelf by Spitsbergen Trough Current (STC) (fig. 1) (Nilsen et al., 2016), which runs nearby from where the transect was taken. A similar situation can be seen in May 2007 (Fig. 8) where TAW is occupying the Kongsfjorden trough. The reason for it to be classified as TAW was because the lower temperature compared to AW, the salinity was still very high which made it stand out as an anomaly. This water mass is generally created due to mixing between AW and Arctic Water (Arw) (Nilsen et al., 2008) Nilsen et al. (2016) describes a correlation between strong cyclones passing through Fram Strait and AW being topographically steered into the STC, from the WSC. On the 23 March of 2007, such a cyclone passed through the Fram Strait going north (Lammert et al., 2009) One could speculate that these events were linked together and that it was the cyclone that caused the AW the flow up on the shelf in the STC, mixing with with Arw and forming the TAW present on the shelf and in Kongsfjorden. Furthermore, in 2014 this was observed again when AW could be seen in Kongsfjorden (Fig. 9) and at the southern point of Spitsbergen, Sørkapp (Fig. 1) With these places being widely apart, it can be speculated that this is likely a major intrusion of AW from the WSC. There is data with CTD-profiles from the mid may in Kongsfjorden, showing TAW occupying most of the Water Colum. There has likely been an exchange of water since AW makes out a big part of the water column shown in Fig. 9, from the end of July.

These events with intrusions of AW entering shelf and fjord have been described because the salinity values (above 35) stood out visually from the “ordinary”. However, there are many other events of AW and TAW intruding upon the shelf and into both Isfjorden and Kongsfjorden. These does not have the same visually striking salinity values as the events that have been mentioned but will stand in strong contrast to the colder water that is otherwise present in fjord and on shelf, as mentioned in Nilsen et al. (2002). These intrusions are also well described in several papers. (Cottier et al., 2007; Nilsen et al., 2008, 2016; Saloranta & Svendsen, 2001; Svendsen et al., 2002)

4.3.2 Low Salinity Events

In 1993 a low salinity anomaly was found in Isfjorden (Fig. 10) and on two stations to the north. In Isfjorden Local Waters (LW) are overlain by warm Surface Waters (SW). The salinity of the SW increases seawards out of the fjord. Most of the glaciers that run into Isfjorden are located on the north side of the fjord, and Nilsen et al. (2008) assumed that glacier ablation and calving are the most important freshwater suppliers to the fjord. Regarding that it seems likely that freshwater input from these glaciers should be of importance. Weather data from Longyearbyen airport (Fig. 1) was examined for temperature, wind, and precipitation (Norwegian Meteorological Institute, 2020) to see if these factors could be the cause of the anomaly. None of these seem to be that far out of the ordinary. Temperature for the first 15 days of august did stand out though, when compared with values from the 1980-2019. There also was quite a bit of wind during these days. However, this was not likely the cause of the anomaly, because CTD-profiles were also available from 1st of august and the situation looked very similar to how it was on the 15th, apart from the surface temperature which had increased.

In 2004 anomalies were found in both Isfjorden and Kongsfjorden at the same time, within a few days from each other. In Isfjorden (Fig. 11) a freshening of the SW towards the north side can be seen. The LW and Winter Cooled Water (WCW) that lies beneath the SW has possibly formed during winter or as it runs by the glacier face and cools, as suggested by (Nilsen et al., 2008; Svendsen et al., 2002). This might have caused some melting, but with this cool water at the glacier face frontal ablation will likely be kept relatively small compared to Fig. 9 for example, where AW extends all the way to the glacier front, as suggested by Luckman et al. (2015). In addition, the temperature data from Longyearbyen Airport did not stand out of the ordinary either (Norwegian Meteorological Institute, 2020). What apparently did stand out from the ordinary this summer, was the distribution of sea ice. According to Promiska et al. (2017) this anomaly may be related with a sea ice event in July 2004. In addition, the amount of fast ice in Isfjorden really stands out during this year, compared to the other years between 2000-2014 (Muckenhuber et al., 2016). Possibly this contribution of meltwater from the sea ice was enough to cause this anomaly in both Isfjorden and Kongsfjorden.

From what been describe above in regards to the low salinity events, these share some common characteristics: In three out of four transects freshening towards the fjord is observed and in one transect freshening towards the side with tidewater glaciers can be seen. This seems to be events that operate on a local scale, but since both 1993 and 2004 anomalies were happening at 2 separate places with relatively great distance from each other, this implies that some larger scale process are causing them.

5. Conclusions

- From the UNIS HD and EN4 database within a distance of 22 km from land, it has been shown that data is sparse from the earlier years and increases towards the end of studied period. A lack of data from the eastern side of Svalbard, compared to the west side, can be seen. Also, data available over a longer period of time for a location, is generally only seen at the western side of Spitsbergen.
- The method used for determining halocline depth was probably not a reliable method for this dataset, because it left a lot of room for subjective interpretation when assigning the depth.
- Salinity anomalies that stood out visually from the norm were observed. Three of these were seen to take place at the same time in locations relatively far away from each other, indicating that the cause of these anomalies were of larger scale.

6. Acknowledgments

Finally, I would like to thank Postdoctoral research fellow Lina Maria Rasmusson, Gothenburg University, for insightful guidance during this project; Professor Hans Linderholm, Gothenburg University, for acting as my examiner; Senior lecturer Mark Johnson, Gothenburg University, for helping me find a project; Professor Riko Noormets, The University Centre in Svalbard, for helping me find salinity data. I would also like to give thanks to my sister, parents, and stepfather for their support.

7. References

Data

Good, S. A., Martin, M. J., & Rayner, N. A. (2013). EN4: Quality controlled ocean temperature and salinity profiles and monthly objective analyses with uncertainty estimates. *Journal of Geophysical Research C: Oceans*, *118*(12), 6704-6716. doi:10.1002/2013JC009067

Norwegian Meteorological Institute, (2020) Seklima. Retrieved 2020-05-26 from <https://seklima.met.no/observations/>

Norwegian Polar Institute, (2020) Norwegian Polar Institute Map Data and Services. Retrieved 2020-05-26 from <https://geodata.npolar.no/>

Skogseth, R., Ellingsen, P., Berge, J., Cottier, F., Falk-Petersen, S., Ivanov, B., ... Vader, A. (2019). UNIS hydrographic database [Data set]. Norwegian Polar Institute. <https://doi.org/10.21334/unis-hydrography>

Literature

Aagaard, K., Folkvik, A., & Hillman, S. R. (1987). The West Spitsbergen Current: disposition and water mass transformation. *Journal of Geophysical Research*, *92*(C4), 3778-3784. doi:10.1029/JC092iC04p03778

Cokelet, E. D., Tervalon, N., & Bellingham, J. G. (2008). Hydrography of the West Spitsbergen Current, Svalbard Branch: Autumn 2001. *Journal of Geophysical Research C: Oceans*, *113*(1). doi:10.1029/2007JC004150

Cottier, F. R., Nilsen, F., Enall, M. E., Gerland, S., Tverberg, V., & Svendsen, H. (2007). Wintertime warming of an Arctic shelf in response to large-scale atmospheric circulation. *Geophysical Research Letters*, *34*(10). doi:10.1029/2007GL029948

Delcroix, T., Alory, G., Cravatte, S., Corregge, T., & McPhaden, M. J. (2011). A gridded sea surface salinity data set for the tropical Pacific with sample applications (1950-2008). *Deep-Sea Research Part I: Oceanographic Research Papers*, *58*(1), 38-48. doi:10.1016/j.dsr.2010.11.002

Durack, P. J., Wijffels, S. E., & Matear, R. J. (2012). Ocean salinities reveal strong global water cycle intensification during 1950 to 2000. *Science*, *336*(6080), 455-458. doi:10.1126/science.1212222

Dyrgerov, M., Bring, A., & Destouni, G. (2010). Integrated assessment of changes in freshwater inflow to the Arctic Ocean. *Journal of Geophysical Research D: Atmospheres*, *115*(12). doi:10.1029/2009JD013060

Flato, G., J. Marotzke, B. Abiodun, P. Braconnot, S.C. Chou, W. Collins, P. Cox, F. Driouech, S. Emori, V. Eyring, C. Forest, P. Gleckler, E. Guilyardi, C. Jakob, V. Kattsov, C. Reason and M. Rummukainen, (2013) Evaluation of Climate Models. In: Climate Change 2013: The Physical Science Basis. Contribution of Working Group I to the Fifth Assessment Report of the Intergovernmental Panel on Climate Change [Stocker, T.F., D. Qin, G.-K. Plattner, M. Tignor, S.K. Allen, J. Boschung, A. Nauels, Y. Xia, V. Bex and P.M. Midgley (eds.)]. Cambridge University Press, Cambridge, United Kingdom and New York, NY, USA.

Fraser, N. J., Skogseth, R., Nilsen, F., & Inall, M. E. (2018). Circulation and exchange in a broad Arctic fjord using glider-based observations. *Polar Research*, *37*(1). doi:10.1080/17518369.2018.1485417

Fofonoff, N. & Millard, R.. (1983). Algorithms for Computation of Fundamental Properties of Seawater. UNESCO Tech. Pap. Mar. Sci.. 44.

Gascard, J.-C., Richez, C. and Rouault, C. (1995). New Insights on Large-Scale Oceanography in Fram Strait: The West Spitsbergen Current. In Arctic Oceanography: Marginal Ice Zones and Continental Shelves

Hanna, E., Huybrechts, P., Janssens, I., Cappelen, J., Steffen, K., & Stenhens, A. (2005). Runoff and mass balance of the Greenland ice sheet: 1958-2003. *Journal of Geophysical Research D: Atmospheres*, *110*(13). doi:10.1029/2004JD005641

Lammert, A., Brummer, B., & Kaleschke, L. (2009). Observation of cyclone-induced inertial sea-ice oscillation in Fram Strait. *Geophysical Research Letters*, *36*(10), L10503-L10503. doi:10.1029/2009GL037197

- Luckman, A., Benn, D. I., Cottier, F., Bevan, S., Nilsen, F., & Inall, M. (2015). Calving rates at tidewater glaciers vary strongly with ocean temperature. *Nature Communications*, 6. doi:10.1038/ncomms9566
- Mathworks, (2020). Griddata. Retrieved 2020-05-26 from <https://se.mathworks.com/help/matlab/ref/griddata.html>
- Melnikov, I. A. (2005). Sea Ice-Upper Ocean Ecosystems and Global Changes in the Arctic. *Russian Journal of Marine Biology*, 31(1), S1-S8. doi:10.1007/s11179-006-0010-8
- Miller, G. H., Alley, R. B., Brigham-Grette, J., Fitzpatrick, J. J., Polyak, L., Serreze, M. C., & White, J. W. C. (2010). Arctic amplification: can the past constrain the future? *Quaternary Science Reviews*, 29(15-16), 1779-1790. doi:10.1016/j.quascirev.2010.02.008
- Muckenhuber, S., Nilsen, F., Korosov, A., & Sandven, S. (2016). Sea ice cover in Isfjorden and Hornsund, Svalbard (2000-2014) from remote sensing data. *Cryosphere*, 10(1), 149-158. doi:10.5194/tc-10-149-2016
- Nilsen, F., Cottier, F., Skogseth, R., & Mattsson, S. (2008). Fjord-shelf exchanges controlled by ice and brine production: The interannual variation of Atlantic Water in Isfjorden, Svalbard. *Continental Shelf Research*, 28(14), 1838-1853. doi:10.1016/j.csr.2008.04.015
- Nilsen, F., Skogseth, R., Vaardal-Lunde, J., & Inall, M. (2016). A Simple Shelf Circulation Model: Intrusion of Atlantic Water on the West Spitsbergen Shelf. *Journal of Physical Oceanography*, 46(4), 1209-1230. doi:10.1175/JPO-D-15-0058.1
- Nummelin, A., Ilicak, M., Li, C., & Smedsrud, L. H. (2016). Consequences of future increased Arctic runoff on Arctic Ocean stratification, circulation, and sea ice cover. *Journal of Geophysical Research: Oceans*, 121(1), 617-637. doi:10.1002/2015JC011156
- Pavlov, A. K., Tverberg, V., Ivanov, B. V., Nilsen, F., Falk-Petersen, S., & Granskog, M. A. (2013). Warming of Atlantic Water in two west Spitsbergen fjords over the last century (1912-2009). *Polar Research*, 32, 1-14. doi:10.3402/polar.v32i0.11206
- Peralta-Ferriz, C., & Woodgate, R. A. (2015). Seasonal and interannual variability of pan-Arctic surface mixed layer properties from 1979 to 2012 from hydrographic data, and the dominance of stratification for multiyear mixed layer depth shoaling. *Progress in Oceanography*, 134, 19-53. doi:10.1016/j.pocean.2014.12.005
- Peterson, B. J., Holmes, R. M., McClelland, J. W., Vorosmarty, C. J., Lammers, R. B., Shiklomanov, A. I., . . . Rahmstorf, S. (2002). Increasing river discharge to the Arctic Ocean. *Science*, 298(5601), 2171-2173. doi:10.1126/science.1077445
- Promiska, A., Cisek, M., & Walczowski, W. (2017). Kongsfjorden and Hornsund hydrography comparative study based on a multiyear survey in fjords of west Spitsbergen. *Oceanologia*, 59(4), 397-412. doi:10.1016/j.oceano.2017.07.003
- Qi, S., Fangli, Q., Zhenya, S., Jiechen, Z., & Xinfang, L. (2018). Projected Freshening of the Arctic Ocean in the 21st Century. *Journal of Geophysical Research: Oceans*, 123(12), 9232-9244. doi:10.1029/2018JC014036
- Rhein, M., S.R. Rintoul, S. Aoki, E. Campos, D. Chambers, R.A. Feely, S. Gulev, G.C. Johnson, S.A. Josey, A. Kostianoy, C. Mauritzen, D. Roemmich, L.D. Talley and F. Wang, (2013) Observations: Ocean. In: Climate Change 2013: The Physical Science Basis. Contribution of Working Group I to the Fifth Assessment Report of the Intergovernmental Panel on Climate Change [Stocker, T.F., D. Qin, G.-K. Plattner, M. Tignor, S.K. Allen, J. Boschung, A. Nauels, Y. Xia, V. Bex and P.M. Midgley (eds.)]. Cambridge University Press, Cambridge, United Kingdom and New York, NY, USA.
- Rudels, B., Anderson, L. G., & Jones, E. P. (1996). Formation and evolution of the surface mixed layer and halocline of the Arctic Ocean. *Journal of Geophysical Research*, 101(C4), 8807-8821. doi:10.1029/96JC00143
- Saloranta, T. M., & Svendsen, H. (2001). Across the Arctic front west of Spitsbergen: High-resolution CTD sections from 1998-2000. *Polar Research*, 20(2), 177-184.
- Sundfjord, A., Kasajima, Y., Kohler, J., Gerland, S., & Torsvik, T. (2017). Effects of glacier runoff and wind on surface layer dynamics and Atlantic Water exchange in Kongsfjorden, Svalbard; a model study. *Estuarine, Coastal and Shelf Science*, 187, 260-272. doi:10.1016/j.ecss.2017.01.015
- Svendsen, H., Beszczynska-Moller, A., Hagen, J. O., Lefauconnier, B., Tverberg, V., Gerland, S., . . . Dallmann, W. (2002). The physical environment of Kongsfjorden-Krossfjorden, and Arctic fjord system in Svalbard. *Polar Research*, 21(1), 133-166. doi:10.1111/j.1751-8369.2002.tb00072.x

Tedesco, M., Fettweis, X., Mote, T., Wahr, J., Alexander, P., Box, J. E., & Wouters, B. (2013). Evidence and analysis of 2012 Greenland records from spaceborne observations, a regional climate model and reanalysis data. *The Cryosphere*, 7(2), 615-630. doi:10.5194/tc-7-615-2013

Weslawski, J. M., Kendall, M. A., Wlodarska-Kowalczyk, M., Iken, K., Kedra, M., Legezynska, J., & Sejr, M. K. (2011). Climate change effects on Arctic fjord and coastal macrobenthic diversity-observations and predictions. *Marine Biodiversity*, 41(1), 71-85. doi:10.1007/s12526-010-0073-9

Software

Mathworks. (2019). MATLAB (Version R2019b) [Computer Software]. Natick, Massachusetts: The MathWorks Inc. Available from <https://mathworks.com/>

Schlitzer, R., (2019). Ocean Data View (Version 5.2.0) [Computer Software]. Available from <https://odv.awi.de/>

Esri. (2019). ArcGIS Desktop (Version 10.7.1) [Computer Software]. United states of America: Esri. Available from <https://esri.com/>

Serif Software. (2014). Affinity Designer (Version 1.7.3) [Computer Software]. England and Wales: Serif Software. Available from <https://affinity.serif.com/en-us/>

Appendix

Data Import

```
%                               Script #1 - Importing data
%   (Green text at the right side of a percent sign are comments)
mappinfo = dir( fullfile('C:\YourFolder', '*.nc') ); % Info about all files
in folder ending with .nc
[antal_filer,~]= size(mappinfo); % total number of files in folder

%   Preallocation of memory (for script to run faster) by creating cell
arrays before looping through all files.
lat = cell(antal_filer, 1);
long = cell(antal_filer, 1);
salinitet = cell(antal_filer, 1);
tryck = cell(antal_filer, 1);
tid = cell(antal_filer, 1);
kalibrering = cell(antal_filer, 1);
temperatur = cell(antal_filer, 1);
djup = cell(antal_filer, 1);

%   The part below loops over all the files and reads the variabels of each
file
%   and add these variabels to cell arrays.

%   Try,catch,and end was added in order to stop error from occurring when
%   salinity, temperature or depth variables were not included in the file.

for K = 1 : antal_filer % for loop iterates over every hole number from 1 to
total number of files.
    fil_nr = fullfile((mappinfo(K).folder),(mappinfo(K).name));

    try
        salinitet{K} = ncread(fil_nr,'PSAL');% for each file (fil_nr) reads the
values of variabel and put them in cell array in row K.
        temperatur{K} = ncread(fil_nr,'TEMP');
        djup{K} = ncread(fil_nr,'FDEP');
    catch
    end
    lat{K} = ncread(fil_nr,'LATITUDE');
    long{K} = ncread(fil_nr,'LONGITUDE');
    tryck{K} = ncread(fil_nr,'PRES');
    tid{K} = ncread(fil_nr,'TIME');
    kalibrering{K} = ncread(fil_nr,'CALIBRATION');
end

%   This part deals with having cell arrays of different sizes; where
%   salinity, temperature and pressure would have XX-XXXX measuremnts while
```

```

% Longitude, Latitude and Date only have 1 entry per cell. This adds
% the number of Longitude, Latitude and Date values in cells to the
% corresponding values of salinity, temperature and pressure. This is done
to be
% able to use the function cell2mat; which converts cell format to
% double. Both cell and double formats have their benefits working with
this data and will be used in
% separate scripts.

[L,W] = size(salinitet); % gives the length of the cell array salinitet
tid_x = cell(L,1); %preallocating memory
long_x = cell(L,1);
lat_x = cell(L,1);
djup_x = cell(L,1);
kalibrering_x = cell(L,1);

for i = 1: antal_filer % for loop, iterates over every hole number from 1 to
number of files.
lengd = size(salinitet{i}); %give the length of the array inside cell 'i'
value_time = tid{i}; % value for time in cell 'i'.
tid_x{i} = (zeros(lengd)+ value_time); %creates an array of zeros with a
length of columns in 'lengd' and adds time value for each row
value_long = long{i};
long_x{i} = (zeros(lengd)+ value_long);
value_lat = lat{i};
lat_x{i} = (zeros(lengd)+ value_lat);
value_kalibrering = kalibrering{i};
value_djup = djup{i};
try
kalibrering_x{i} = (zeros(lengd)+ value_kalibrering);
djup{i} = (zeros(lengd)+ value_djup);
catch
kalibrering_x{i} = zeros(lengd);
djup_x{i} = zeros(lengd);
end
end

% In preparation of script #2

nydata = [salinitet,temperatur,tryck,lat,long,tid]; % Creating a matrix with
variables from the imported data.
tomma_rader = any(cellfun(@isempty, nydata), 2); %Finding the cells that
doesn't have any data
nydata(tomma_rader,:) = []; % Delete these rows

% The part beneath deletes the nan values inside the cells of salinity and
% then removes the corresponding values for pressure.
[langd,bredd] = size(nydata);

```



```

bada_kolumner = cell(langd,2); % creating cell array with same amount of rows
as in nydata and 2 columns.
for i = 1 : langd
    kolumn1 = nydata{i,1}; % defining kolumn1 as an array with the contents
of the cell in row i, column 1 of nydata.
    kolumn2 = nydata{i,2}; % defining kolumn2 as an array with the contents
of the cell in row i, column 2 of nydata.
    nan_varden = isnan(kolumn1); % locating NaN values
    kolumn1(nan_varden) = []; % remove NaN values from kolumn1
    kolumn2(nan_varden) = []; % remove corresponding NaN values from kolumn1
    bada_kolumner{i,1} = kolumn1;
    bada_kolumner{i,2} = kolumn2;

end
Script3_data = [bada_kolumner,nydata(:,3:5)];

%           In preparation of Script #3

latlongtime = [salinitet,tryck,lat_x,long_x,tid_x]; %puts cell arrays
together in a matrix

rad_tomma_varden = any(cellfun(@isempty, latlongtime), 2); %Find rows with
empty values
latlongtime(rad_tomma_varden,:) = []; %Delete these rows
Skript2_data = cell2mat(latlongtime); %converts cell array in to double
array.

rader_nan = any(isnan(Skript2_data),2); % Finds the rows with nan values.
(lots of the salinity measurements where listed as NaN (not a number))
Skript2_data(rader_nan,:) = []; % removes rows with nan values.

```

Script #2

```

%           Script #2 - 2D diagrams of salinity and depth.
close all

Innehall_mapp =
dir(fullfile('C:\Users\darin\Documents\MATLAB\Analysdata2D_medtemp',
'*.mat')); %info about files in folder that end in .mat
spara = cell(length(Innehall_mapp),1);

%loops trough all data for all files in folder and selects data that fits
%in latitude and longitude interval.
for k = 1:length(Innehall_mapp)
    data1 = struct2cell(load(Innehall_mapp(k).name));%Loads 'k' file and
converts it to cell format.
    data = data1{1,1}; %getting contents of cell
    [l, ~] = size(data); % size of rows and column

```

```

Z = cell(1,6);
for i = 1 : 1
    x = data{i,4};
    y = data{i,5};
    if (Co(1,1) <x)&& (x< Co(1,2)) && (Co(1,3) < y)&&(y < Co(1,4))%
Lat.min<x<Lat.max AND Lon.min<y<Lon.max. Determines if a point is within these
intervals.
        Z{i,1} = data{i,1};%if it is within the interval it adds the data to Z
        Z{i,2} = data{i,2};
        Z{i,3} = data{i,3};
        Z{i,4} = data{i,4};
        Z{i,5} = data{i,5};
        Z{i,6} = data{i,6};
    end
end

Q= any(cellfun(@isempty, Z), 2);%Finds empty rows(There will be empty rows
where the data didn't fall inside the interval.)
Z(Q,:)= []; %Delete empty rows.
spara{k} = Z; %saves data in 'spara' for each iteration of K

end

a = spara{1,1};
b = spara{2,1};
c = spara{3,1};
d = spara{4,1};
e = spara{5,1};
f = spara{6,1};

X =[a;b;c;d;e;f];

D = X(:,3);%depth
S = X(:,1); %salinity
t1 = cell2mat(X(:,6)); %days since 1950-01-01
t2 = 19500101;
t3 = datetime(t2,'ConvertFrom','yyyymmdd');
t4 = juliandate(t3);
t5 = t1 + t4;
T = datetime(t5,'convertfrom','juliandate'); % in datetime format

Lat = round(cell2mat(X(:,4)),2);
Long =round(cell2mat(X(:,5)),2);
[1,W] = size(X);

% For loop that makes a 2D plot and saves it to a file for each
% iteration(with Date,Lon and Lat).

```

```

for i = 1 : l
    x = S{i,1};
    y = D{i,1};
    %    y = (-1) * y1;
h = plot(x,y,'r-o','DisplayName','CTD-Measurements');
lgd = legend(h,'Location','southwest');
xlabel('Salinity [psu]')
ylabel('Depth [m]')
xlim([27 36]);
set(gca, 'YDir','reverse')
grid on
grid minor
title(sprintf('Date:%s Lat:%.2f Long:%.2f', string(T(i)), Lat(i), Long(i)));
saveas(gcf, ['Salthalt_i' num2str(i) '.png'])%saves image
end

```

Script #3

```

%                               Script #3 - Surface plots

close all
Innehall_mapp = dir(fullfile('C:\Users\darin\Documents\MATLAB\analysdata_3D',
'*.mat')); %info about files in folder that end in .mat
spara = cell(length(Innehall_mapp),1);

for k = 1:length(Innehall_mapp)
    fil_innehall = cell2mat(struct2cell(load(Innehall_mapp(k).name)));%Loads
'k' file and converts it to double format.
    [langd, bredd] = size(fil_innehall); % size of rows and columns
    addera = zeros(langd,6); % preallocates memory
    for i = 1 : langd
        x = fil_innehall(i,4);
        y = fil_innehall(i,5);
        La_min = Co(1,1);
        La_max = Co(1,2);
        Lo_min = Co(1,3);
        Lo_max = Co(1,4);

        if ( La_min <x)&& (x< La_max) && (Lo_min < y)&&(y < Lo_max)
            addera(i,:) = fil_innehall(i,:);
        end
    end

    omrade = addera(any(adder,2),:); % export rows that is not all zero
    cell = num2cell(omrade); %converts to cell format
    spara{k} = cell; % saves output of each file as a cell in row 'k'.

```

```

end

a = cell2mat(spara{1,1}); %convert each cell back to a matrix in double
format.
b = cell2mat(spara{2,1});
c = cell2mat(spara{3,1});
d = cell2mat(spara{4,1});
e = cell2mat(spara{5,1});
f = cell2mat(spara{6,1});
g = cell2mat(spara{7,1});
h = cell2mat(spara{8,1});
x = [a;b;c;d;e;f;g;h];

datum1 = 19500101;
datum2 = datetime(datum1,'ConvertFrom','yyyymmdd');
datum = juliandate(datum2);
bada_datum = x(:,6) + datum; %adds julian time to 1950101 and days since
1950101(wich the data was deliverd in) together to be able to convert time
gregorian calendar.

tid2 = datetime(bada_datum,'convertfrom','juliandate'); %converts time
Datetime format.

tid_v = datevec(tid2);%datevector format
vektortid = tid_v(:,1:3); % time in year months and days
tid_y = yyyymmdd(tid2); %yyyymmdd format
tid_d = datenum(tid2); %datenum format
y = [x(:,1:5),tid_d(:,1),tid_v(:,2)]; %adds the converted datenum time to a
new matrix with the other variables.
%% For loop below removes profiles taken inte wintermonths

for j = 1 : length(y)
    manad = y(j,7);
    if ( 0<manad)&& (manad< 13) %Select months between interval
        ym(j,:) = y(j,:);
    end
end
Ym = ym(any(ym,2),:);

X1 = Ym(:,6);
X2 = (-1) * Ym(:,3);
X3 = Ym(:,1);

tryck_mesh = 0 :-1:min(X2) ;
datum_mesh = min(X1) :20: max(X1) ;

```

```

tryck_mesh_t = tryck_mesh'; % Transposing to a columnvector.
X4 = X3 + 2 ; % Elevates the scatterplot above the surface.

[xq,yq] = meshgrid(datum_mesh,tryck_mesh_t); % creates a grid with input
variables, in which datum_mesh is copied for all the rows in xq and
tryck_mesh_t is copied for all columns in yq.

vq = griddata(X1,X2,X3,xq,yq);% Creates a surface that is interpolated
between the query points, xq and yq. The interpolated surface always passes
through the X1,X2 and X3 points.
mesh(xq,yq,vq),hold on % Plots vq as surface in relation to xq and yq in a
diagram.

h = scatter3(X1,X2,X4,'fill','black','SizeData',7,'DisplayName','CTD-
Measurements'); hold off %adds a scatterplot to the diagram
datetick('x','yyyy','keeplimits')
cb = colorbar;
title(cb,'Salinity [psu]')
xlabel('Year')
ylabel('depth [m]')
zlabel('Salinity [psu]')
set(gca,'FontSize',20)
lgd = legend(h,'Location','southeast');

```

Script #4

```

%                               Script #4 - Intersect Area

close all
Innehall_mapp = dir(fullfile('C:\Users\darin\Documents\MATLAB\analysdata_3D',
'*.mat')); %info about files in folder that end in .mat
spara = cell(length(Innehall_mapp),1);

for k = 1:length(Innehall_mapp)
    fil_innehall = cell2mat(struct2cell(load(Innehall_mapp(k).name)));%Loads
'k' file and converts it to double format.
    [langd, bredd] = size(fil_innehall); % size of rows and columns
    addera = zeros(langd,6); % preallocates memory
    for i = 1 : langd
        x = fil_innehall(i,4);
        y = fil_innehall(i,5);
        La_min = Co(1,1);
        La_max = Co(1,2);
        Lo_min = Co(1,3);
        Lo_max = Co(1,4);

        if ( La_min < x) && (x < La_max) && (Lo_min < y) && (y < Lo_max)

```



```

    addera(i,:) = fil_innehall(i,:);
end
end

omrade = addera(any(adder,2),:); % export rows that is not all zero
cell = num2cell(omrade); %converts to cell format
spara{k} = cell; % saves output of each file as a cell in row 'k'.

end

a = cell2mat(spara{1,1}); %convert each cell back to a matrix in double
format.
b = cell2mat(spara{2,1});
c = cell2mat(spara{3,1});
d = cell2mat(spara{4,1});
e = cell2mat(spara{5,1});
f = cell2mat(spara{6,1});
g = cell2mat(spara{7,1});
h = cell2mat(spara{8,1});
x = [a;b;c;d;e;f;g;h];

datum1 = 19500101;
datum2 = datetime(datum1,'ConvertFrom','yyyymmdd');
datum = juliandate(datum2);
bada_datum = x(:,6) + datum; %adds julian time to 1950101 and days since
1950101(wich the data was deliverd in) together to be able to convert time
gregorian calendar.

tid2 = datetime(bada_datum,'convertfrom','juliandate'); %converts time
Datetime format.
tid_v = datevec(tid2);%datevector format
vektortid = tid_v(:,1:3); % tiden i år, månad, dagar
tid_y = yyyymmdd(tid2); %yyyymmdd format
tid_d = datenum(tid2); %datenum format
Ym = [x(:,1:5),tid_d(:,1),tid_v(:,2),tid_y]; %adds the converted datenum time
to a new matrix with the other variables.
%% For loop below removes profiles taken into wintermonths

    Ymd = zeros(length(Ym),8);
    for p = 1 : length(Ym)
        datumet = Ym(p,8);
        if (20140509 < datumet) && (datumet < 20140511) % Searches for the profiles
within a specific date interval.
            Ymd(p,:) = Ym(p,:);
        end
    end
end
Intersect_area = Ymd(any(Ymd,2),:);

```